Contribution from the Departments of Chemistry, Brown University, Providence, Rhode Island 02912, and University of Otago, Dunedin, New Zealand

Paramagnetic Organometallic Molecules. 16. ESR Studies of Cobalt Acetylene π Complexes: A New Class of Fluxional Organocobalt Radicals[1]

LOUIS V. CASAGRANDE,[2a] TAICHENG CHEN,[2a,3] PHILIP H. RIEGER,*[2a] BRIAN H. ROBINSON,[2b] JIM SIMPSON,[2b] and STEVEN J. VISCO[2a]

Received November 8, 1983

ESR studies are reported on 19 radicals of the general formula $(R_2C_2)Co(CO)_{3-x}L_x$ where L is a phosphine, phosphite, or arsine and $x = 0$–3. The radicals are obtained by reduction of THF solutions of acetylene-bridged dicobalt clusters, $R_2C_2Co_2(CO)_{6-x}L_x$, in the presence of excess ligand L and, for $x = 2$ or 3, are long-lived at room temperature. ESR line width studies show the radicals $(Ph_2C_2)Co(CO)[P(OMe)_3]_2$ to be very rapidly fluxional ($\tau = 2.2 \times 10^{-11}$ s at 290 K) with instantaneously nonequivalent phosphite ligands. Analysis of the frozen-solution ESR spectrum of $(t\text{-}Bu_2C_2)Co(CO)_2P\text{-}n\text{-}Bu_3$ permits detailed characterization of the semioccupied molecular orbital. A pseudo-square-planar molecular structure can be inferred from the ESR results.

Recent work[4] has shown that polynuclear metal carbonyl compounds with a metal–metal backbone can generally be reduced to anions in which the formal 18-electron electronic configuration is exceeded. This redox property arises because there is a relatively accessible LUMO in the neutral species that is centered on the metal cluster backbone.[5] A detailed study of the radical anions can provide important information on the electronic structure of the polynuclear carbonyl as well as the feasibility of using these species in synthetic and catalytic reactions.

We have reported ESR[6,7] and electrochemical studies[8] of the redox properties of the dinuclear acetylene-bridged compounds $(RC_2R')Co_2(CO)_6$. These studies led to the discovery[8,9] of electron-transfer chain-catalyzed (ETC) nucleophilic substitution in organo transition metal clusters. One of the factors that determines the efficiency of the ETC reactions with the acetylene compounds is the importance of the alternative reaction mode to nucleophilic substitution of the radical anions—namely, fragmentation of the radical anions to produce the mononuclear organocobalt radicals $(RC_2R')Co(CO)_{3-x}L_x$. This new class of radical is produced as summarized in Scheme I.[8] When L = CO, only the fragmentation process leads to net reaction. However, since $E_3 > E_1$ in this case, monocobalt radicals formed near the electrode are immediately reduced and an overall 2-electron process is observed. However, when L is a phosphine, phosphite, or arsine, both E_2 and E_3 are more negative than E_1 and good yields of the monocobalt radicals and the substituted dicobalt clusters are obtained.

In this paper, we report a variety of ESR experiments designed to characterize these monocobalt radicals and to deduce their electronic and molecular structures.

Experimental Section

X-Band ESR spectra were recorded on Varian E-4 or Bruker ER-220D spectrometers equipped with variable-temperature units and microwave-frequency counters. The Bruker spectrometer was interfaced to an ASPECT-2000 computer. Radicals were prepared by reduction of tetrahydrofuran (THF) solutions of $(RC_2R')Co_2(CO)_6$ (R, R′ = Ph, *t*-Bu, CF_3; R = CF_3, R′ = $Si(CH_3)_3$, 0.01 M) and tetra-*n*-butylammonium perchlorate, 0.10 M, by in situ electrolysis.[7] The sources and/or preparations of the chemicals used in this work are described elsewhere.[8]

Scheme I

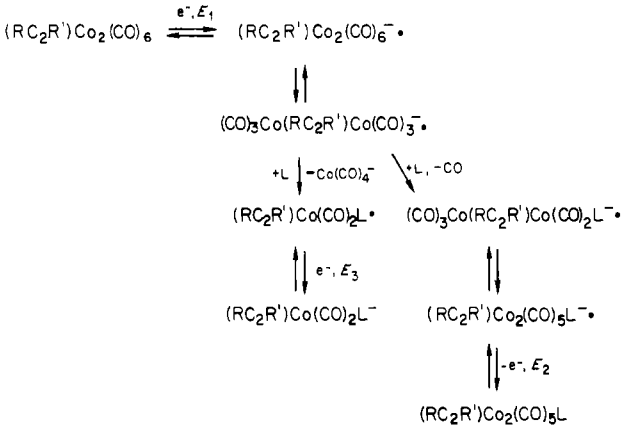

Results

Isotropic ESR Spectra. ESR spectra of the anion radicals $(RC_2R')Co_2(CO)_6^{-\bullet}$ were observed when THF solutions of the parent molecules were reduced electrolytically in a cell maintained at −60 °C in the ESR cavity.[6,7] Radical anions had lifetimes of 1 min or more at this temperature, and well-resolved spectra were obtained. These spectra were the subject of an earlier report.[7]

When electrolysis of solutions of $(R_2C_2)Co_2(CO)_6$ (R = Ph, *t*-Bu) was carried out at higher temperatures, −30 to −50 °C, an 8-line ESR spectrum was obtained, apparently arising from hyperfine coupling to a single ^{59}Co nucleus ($I = {}^7/_2$). These spectra, which were always weak and required prolonged electrolysis to be observable, are assigned to the radicals $(R_2C_2)Co(CO)_3$. These radicals have lifetimes of a few minutes at −50 °C; no ESR signal was observed on electrolysis at temperatures higher than −30 °C. Reduction of $(Ph_2C_2)Co_4(CO)_{10}$ under similar conditions gave a weak 8-line spectrum identical with that obtained from $(Ph_2C_2)Co_2(CO)_6$. The anion radicals of $[CF_3C_2Si(CH_3)_3]Co_2(CO)_6$ and $[(CF_3)_3C_2]Co_2(CO)_6$ were relatively stable; no 8-line spectrum was ever observed on electrolysis of these compounds.

Reduction of the R = *t*-Bu compound in the presence of excess P-*n*-Bu_3 or $P(OMe)_3$ at temperatures from −50 to +10 °C gave 16-line spectra (hyperfine coupling to one ^{59}Co and one ^{31}P nuclei, $I = {}^1/_2$) that are assigned to the radicals $(t\text{-}Bu_2C_2)Co(CO)_2L$. The spectra appeared immediately on

(1) Part 15: Huffadine, A. S.; Peake, B. M.; Robinson, B. H.; Simpson, J. *Aust. J. Chem.*, in press.
(2) (a) Brown University. (b) University of Otago.
(3) ACS-PRF Summer Fellow, 1982.
(4) Peake, B. M.; Rieger, P. H.; Robinson, B. H.; Simpson, J. *Inorg. Chem.* **1981**, *20*, 2540–2543 and references therein.
(5) Lauher, J. W. *J. Am. Chem. Soc.* **1978**, *100*, 5305–5315.
(6) Dickson, R. S.; Peake, B. M.; Rieger, P. H.; Robinson, B. H.; Simpson, J. *J. Organomet. Chem.* **1979**, *172*, C63–C65.
(7) Peake, B. M.; Rieger, P. H.; Robinson, B. H.; Simpson, J. *J. Am. Chem. Soc.* **1980**, *102*, 156–163.
(8) Arewgoda, M.; Rieger, P. H.; Robinson, B. H.; Simpson, J.; Visco, S. J. *J. Am. Chem. Soc.* **1982**, *104*, 5633–5640.
(9) Bezems, G. J.; Rieger, P. H.; Visco, S. J. *J. Chem. Soc., Chem. Commun.* **1981**, 265–266. Arewgoda, M.; Robinson, B. H.; Simpson, J. *Ibid.* **1982**, 284–285. Bruce, M. I.; Kehoe, D. C.; Matisons, J. G.; Nicholson, B. K.; Rieger, P. H.; Williams, M. L. *Ibid.* **1982**, 442–444.

0020-1669/84/1323-2019$01.50/0

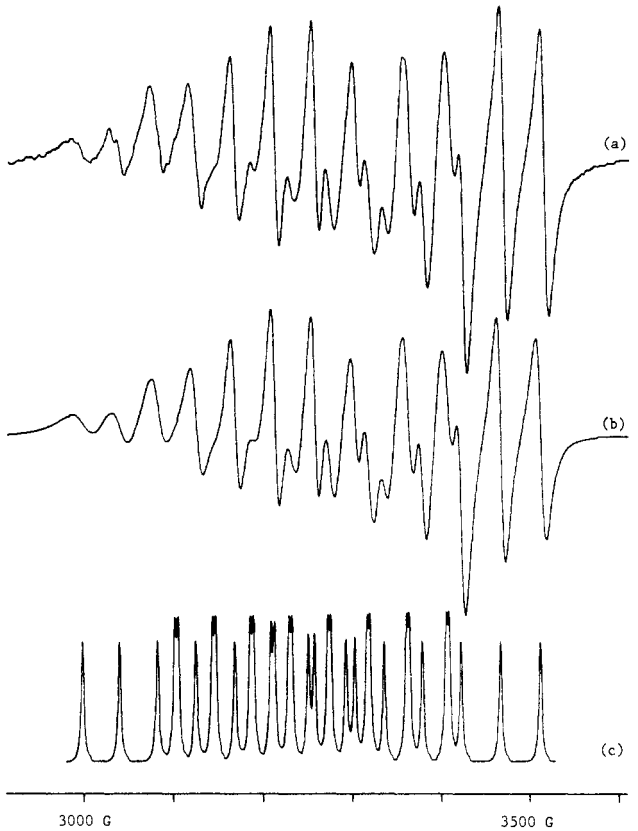

Figure 1. ESR spectra of $(Ph_2C_2)Co(CO)[P(OMe)_3]_2$ at 270 K: (a) experimental; (b) simulated; (c) simulated constant-width absorption spectrum (stick spectrum) showing second-order splittings of the $m_p = 0$ lines.

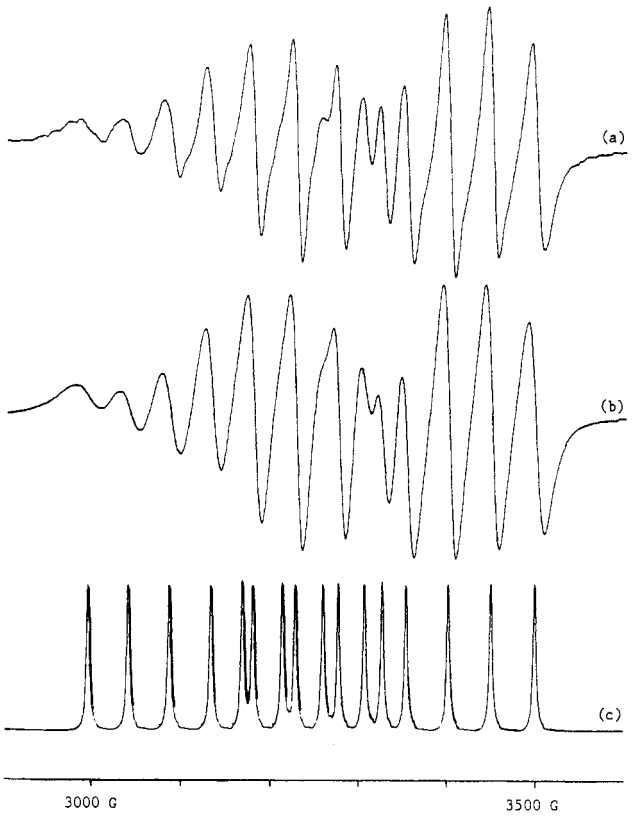

Figure 2. ESR spectra of $(Ph_2C_2)Co(CO)_2[P(OMe)_3]$ at 260 K: (a) experimental; (b) simulated; (c) simulated constant-width absorption spectrum (stick spectrum).

commencement of electrolysis and grew in intensity on continued passage of current. These radicals were unstable at higher temperatures so that a steady-state ESR intensity was rapidly achieved on electrolysis at −10 °C or above.

Reduction of the R = Ph compound in the presence of excess PPh_3, P-*n*-Bu_3, $P(C_6H_{11})_3$, or $P(OPh)_3$ similarly gave 16-line spectra, and with excess $AsPh_3$, a 32-line spectrum was obtained (coupling to one ^{59}Co and one ^{75}As nuclei, $I = {}^3/_2$). With a 100-fold excess of $P(OMe)_3$ or $P(OEt)_3$, 24-line spectra (Figure 1a) were obtained (coupling to one ^{59}Co and two ^{31}P nuclei) that are assigned to $(Ph_2C_2)Co(CO)L_2$. With a stoichiometric amount of $P(OMe)_3$, reduction at −30 °C gave only the monosubstituted radical (Figure 2). With a 10-fold excess of $P(OMe)_3$, a mixture of mono- and disubstituted radicals was obtained. Reduction of $(Ph_2C_2)Co_2(CO)_{6-x}[P(OMe)_3]_x$ (x = 1, 2) without added $P(OMe)_3$ also gave the disubstituted radical. The disubstituted radicals are considerably more stable than the unsubstituted or monosubstituted species with lifetimes of several hours at +30 °C.

Electrolysis of $[CF_3C_2Si(CH_3)_3]Co_2(CO)_6$ or $[(CF_3)_2C_2]Co_2(CO)_6$ in the presence of $P(OMe)_3$ at −30 °C gave the usual anion radical speectra, but after prolonged electrolysis at −10 °C, weak spectra were observed that exhibited hyperfine coupling to a single ^{59}Co and to two ^{31}P nuclei. The dinuclear anion radicals have lifetimes of 1 min or more at this temperature, and their spectra are easily observed in the absence of $P(OMe)_3$.

Reduction of $[(CF_3)_2C_2]Co_2(CO)_3[P(OMe)_3]_3$ or $(Ph_2C_2)Co_2(CO)_3[P(OMe)_3]_3$ at room temperature in the presence of excess $P(OMe)_3$ gave 32-line spectra (coupling to one ^{59}Co and three equivalent ^{31}P nuclei) that are assigned to $(R_2C_2)Co[P(OMe)_3]_3$.

Reduction of the R = Ph compound in the presence of an excess of the bidentate ligands $Ph_2PCH_2CH_2PPh_2$, $Ph_2AsCH_2CH_2AsPh_2$, or $Ph_2PCH_2CH_2AsPh_2$ give, respectively, 24-, 32-, and 16-line spectra. Thus, in contrast to the $Ph_2PCH_2CH_2PPh_2$ species in which coupling to both donor atoms is observed, coupling to only one donor atom (^{75}As and ^{31}P, respectively) is shown by the other two species (Table I). These three radicals have stabilities characteristic of other disubstituted species, and the latter two give spectra with broader lines suggestive of unresolved ^{75}As coupling. We have therefore assigned disubstituted structures to all three and conclude that the radicals have two types of substitution sites, one of which results in a large ligand coupling and the other a much smaller coupling. When one or both of the ligand

Table I. Isotropic ESR Parameters

radical	$\langle g \rangle^a$	$\langle A^{Co} \rangle^b$	$\langle A^X \rangle^c$
$(Ph_2C_2)Co(CO)_3$	2.060	49.2	
$(t\text{-}Bu_2C_2)Co(CO)_3$	2.057	50.6	
$(Ph_2C_2)Co(CO)_2P\text{-}n\text{-}Bu_3$	2.059	43.0	112.0 (1 P)
$(Ph_2C_2)Co(CO)_2P(c\text{-}C_6H_{11})_3$	2.064	41.5	110.6 (1 P)
$(Ph_2C_2)Co(CO)_2PPh_3$	2.07[d]	44.3	114.1 (1 P)
$(Ph_2C_2)Co(CO)_2P(OMe)_3$	2.061	45.4	166.3 (1 P)
$(Ph_2C_2)Co(CO)_2P(OPh)_3$	2.06[d]	46.2	170.5 (1 P)
$(Ph_2C_2)Co(CO)_2AsPh_3$	2.076	34.6	135.4 (1 As)
$(t\text{-}Bu_2C_2)Co(CO)_2P\text{-}n\text{-}Bu_3$	2.060	47.8	111.3 (1 P)
$(t\text{-}Bu_2C_2)Co(CO)_2P(OMe)_3$	2.057	48.0	165.3 (1 P)
$[CF_3C_2Si(CH_3)_3]Co(CO)[P(OMe)_3]_2$	2.066	43.3	102.9 (2 P)
$[(CF_3)_2C_2]Co(CO)[P(OMe)_3]_2$	2.070	43.3	97.3 (2 P)
$(Ph_2C_2)Co(CO)[P(OEt)_3]_2$	2.064	43.0	105.0 (2 P)
$(Ph_2C_2)Co(CO)[P(OMe)_3]_2$	2.061	43.4	105.1 (2 P)
$(Ph_2C_2)Co(CO)[Ph_2PCH_2CH_2PPh_2]$	2.073	40.5	67.0 (2 P)
$(Ph_2C_2)Co(CO)[Ph_2AsCH_2CH_2AsPh_2]$	2.075	35.6	135.4 (1 As)
$(Ph_2C_2)Co(CO)[Ph_2PCH_2CH_2AsPh_2]$	2.064	43.1	113.2 (1 P)
$[(CF_3)_2C_2]Co[P(OMe)_3]_3$	2.074	38.8	77.4 (3 P)
$(Ph_2C_2)Co[P(OMe)_3]_3$	2.068	45.0	78.8 (3 P)

[a] ±0.002, except where noted. [b] Units of 10^{-4} cm^{-1}; uncertainty, ±0.2. [c] Units of 10^{-4} cm^{-1}; uncertainty, ±0.5. [d] ±0.01.

atoms is As, exchange between the two sites is slow, but when two or three phosphorus ligands are present, exchange is fast enough that the ^{31}P nuclei appear equivalent. Line width effects expected from this exchange process are in fact observed and are discussed below.

Line positions were fitted to a second-order solution to the spin Hamiltonian[10] to give the isotropic g values and hyperfine coupling constants shown in Table I.

In most cases, spectra were recorded at several temperatures. The g values and cobalt coupling constants are independent of temperature within experimental error, as are the phosphorus couplings in the di- and trisubstituted radicals. The phosphorus couplings in the monosubstituted radicals, on the other hand, are somewhat temperature dependent, with a temperature coefficient of about −0.1%/K. The coupling constants in Table I refer in every case to the best resolved spectrum obtained usually at or above 0 °C.

ESR Line Width Studies. Incomplete averaging of the **g** and hyperfine tensor anisotropies is expected to result in line broadening that is in general expressable as a power series in the nuclear spin quantum numbers[10-12] (eq 1), where m_i is the

$$\text{width} = \alpha + \sum\beta_i m_i + \sum\gamma_i m_i^2 + \sum_{i\neq j}\epsilon_{ij} m_i m_i \qquad (1)$$

nuclear spin quantum number of the ith nucleus. The parameter α includes the line width contributions that are independent of m_i, including a term proportional to $(g_\parallel - g_\perp)^2\tau_R$ where τ_R is the rotational correlation time. The parameters β_i are proportional to the products of **g** and hyperfine tensor anisotropies, $(g_\parallel - g_\perp)(A_\parallel^i - A_\perp^i)\tau_R$, whereas γ_i and ϵ_{ij} are related primarily to the hyperfine tensor anisotropies, $\gamma_i \propto (A_\parallel^i - A_\perp^i)^2\tau_R$ and $\epsilon_{ij} \propto (A_\parallel^i - A_\perp^i)(A_\parallel^j - A_\perp^j)\tau_R$. In the spectra at hand, we observe a decrease in line width with increasing magnetic field indicating that β_{Co} is important and that this parameter has the same sign as $\langle A^{Co}\rangle$. Although γ_{Co} is significant, the spectra of the monosubstituted radicals show little or no variation in line width with ^{31}P or ^{74}As quantum numbers, consistent with the expectation that the ^{31}P and ^{75}As hyperfine tensors are nearly isotropic.

In spectra with two (or three) ^{31}P couplings, on the other hand, the line widths are strongly dependent on m_P, but with β_P negligible and γ_P negative. That is, the $m_P = \pm 1$ (or $\pm^3/_2$) lines are sharper than the corresponding $m_P = 0$ (or $\pm^1/_2$) lines. This behavior cannot be explained by incomplete averaging of anisotropies; it must be due to exchange of ^{31}P nuclei between coordination sites with different hyperfine couplings. If we assume that, in the disubstituted radicals, one ^{31}P has a large coupling and the other small (one large and two small couplings in the trisubstituted radicals), then the contribution to the width (in Gauss) of the $m_P = 0$ (or $\pm^1/_2$) lines should be given by[11] (2), where A_A and A_B are the coupling constants

$$-\gamma_P = \frac{4\pi hc^2}{3g\mu_B{}^{1/2}} p_A p_B \tau (A_A - A_B)^2 \qquad (2)$$

at sites A and B (in cm^{-1}), p_A and p_B are the probabilities that the sites will be occupied by a phosphite ligand, and τ is the mean lifetime, $\tau = \tau_A\tau_B/(\tau_A + \tau_B)$. Note that because of the form of eq 1, the correct m_I-independent line width is $\alpha + \gamma_P$.

Direct measurement of line widths in these spectra is difficult because of extensive overlapping of components, and the usual manual techniques were unsuccessful. Accordingly, a nonlinear least-squares program, written in PASCAL for the ASPECT-2000 computer, was developed that fitted a simulated spectrum to a digitized experimental spectrum with α, β_{Co}, γ_{Co}, and γ_P as adjustable parameters. The simulation used values of $\langle g\rangle$, $\langle A^{Co}\rangle$, and $\langle A^P\rangle$, which were separately obtained from a least-squares analysis of the line positions in the same spectrum. Average fitting errors ranged around 0.3%, and the resulting simulated spectra are very good matches to the experimental spectra (Figure 1).

Table II. Line Width Parameters for $(Ph_2C_2)Co(CO)[P(OMe)_3]_2$[a]

T/K	$\alpha + \gamma_P$	β_{Co}	γ_{Co}	γ_P	$10^{11}\tau$[b]/s
290	13.8	−2.03	0.48	−3.06	2.2
270	14.1	−2.77	0.68	−4.67	3.3
250	17.0	−3.81	0.90	−9.25	6.5

[a] Line width parameters, in units of Gauss, refer to the width between extrema of first derivative lines. [b] Mean lifetime computed from γ_P and an estimate of $(A_A - A_B)^2$. See text.

Spectra of $(Ph_2C_2)Co(CO)[P(OMe)_3]_2$ at 250, 270, and 290 K were analyzed in this way; the line width parameters are given in Table II. The parameters $\alpha + \gamma_P$, β_{Co}, and γ_{Co} are seen to increase with decreasing temperature as expected if the line widths are due primarily to slow tumbling of the radicals in solution, $\tau_R \propto \mu/T$. Indeed the temperature variation of the parameters β_{Co} and γ_{C3} give Arrhenius activation energies of 9.5 ± 0.3 and 9.4 ± 0.7 kJ mol^{-1}, respectively. The temperature variation of $\alpha + \gamma_P$ is considerably less, suggesting other major contributions that are independent of m_I.[13]

In order to determine τ from the measured line width contributions, we must estimate the couplings at the two sites. We can approximate these couplings by comparing the ^{31}P couplings in $(Ph_2C_2)Co(CO)_{3-x}[P(OMe)_3]_x$ for $x = 2$ and 3 (see Table I). If A_A is the coupling at site A and A_B is the coupling at site B and we assume that there is a site A phosphite in both cases, one site B ligand for $x = 2$, and two site B ligands for $x = 3$, then the average couplings for $x =$ 2 and 3 are

$$A_2 = {}^1/_2(A_A + A_B) \qquad (3a)$$

$$A_3 = {}^1/_3(A_A + 2A_B) \qquad (3b)$$

Fitting the experimental values of A_2 and A_3 to eq 3 gives $A_A = 184 \times 10^{-4}$ cm^{-1} and $A_B = 26 \times 10^{-4}$ cm^{-1}.

Substitution of these coupling constants into eq 2, together with the experimental values of γ_P, gives the values of τ given in Table II. The temperature dependence of τ corresponds to an activation energy of 17 ± 2 kJ mol^{-1}.

The estimate of the site A coupling is about 10% larger than the ^{31}P coupling in $(Ph_2C_2)Co(CO)_2[P(OMe)_3]$, suggesting that the monosubstituted radicals may exist as an equilibrium mixture of isomers with phosphorus ligands at sites A and B. This is probably the reason for the small temperature dependence of the ^{31}P coupling in monosubstituted radicals.

Frozen-Solution ESR Spectra. ESR spectra of frozen THF solutions of the monocobalt radicals, generated as described above, varied considerably in resolution and in signal-to-noise ratio and were often complicated by low-intensity spectral features apparently due either to other radical species or to other radical conformations. The best quality spectrum was that of $(t\text{-}Bu_2C_2)Co(CO)_2P\text{-}n\text{-}Bu_3$, and this spectrum was analyzed in detail. The spectrum, shown in Figure 3a, shows a fairly obvious series of features, spaced about 100 G apart, which correspond to the largest component of the ^{59}Co hyperfine tensor. The corresponding ^{31}P hyperfine tensor component is also approximately 100 G. A second series of features can be identified with a ^{59}Co coupling of about 60 G and a ^{31}P coupling of about 110 G. Several features can be

(10) Wilson, R.; Kivelson, D. *J. Chem. Phys.* **1966**, *44*, 154–168.
(11) Fraenkel, G. K. *J. Phys. Chem.* **1967**, *71*, 139–171.
(12) Peake, B. M.; Rieger, P. H.; Robinson, B. H.; Simpson, J. *Inorg. Chem.* **1979**, *18*, 1000–1005.

(13) Contributions to α from the spin–rotation interaction and unresolved hyperfine coupling are probably most important. See ref 10–12.

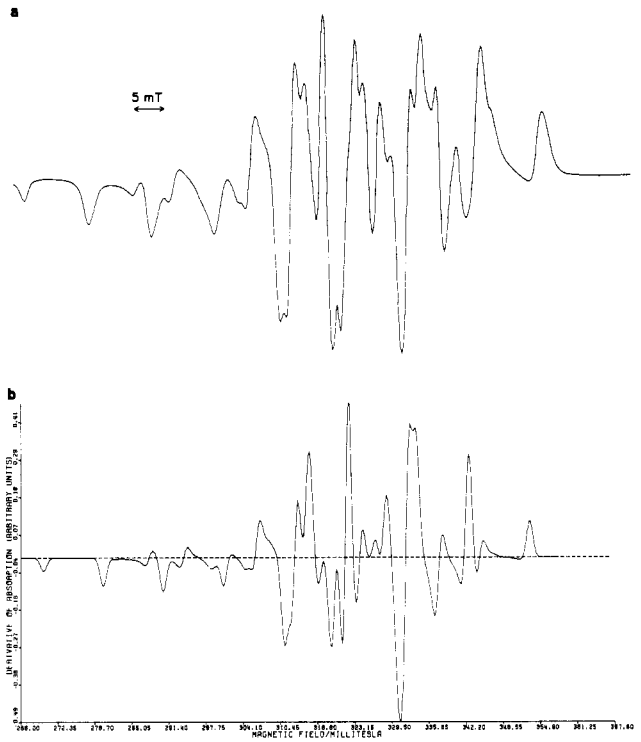

Figure 3. ESR spectra of $(t\text{-}Bu_2C_2)Co(CO)_2P\text{-}n\text{-}Bu_3$ at 120 K: (a) experimental; (b) simulated.

Table III. Anisotropic ESR Parameters for $(t\text{-}Bu_2C_2)Co(CO)_2P\text{-}n\text{-}Bu_3$

i	g_i	$10^4A_i^{Co}$/ cm^{-1}	$10^4A_i^{P}$/ cm^{-1}
1	2.095	−102.0	100.2
2	2.063	−62.3	106.5
3	2.022	+2.07	127.2

identified that apparently correspond to a third series, but quantum number assignments cannot be made directly for these. With two components each of the **g** tensor and of the ^{59}Co and ^{31}P hyperfine tensors established, the third components can be estimated from the isotropic parameters and assignments of these features can be made. With about 20 features unambiguously assigned, the spectrum was subjected to least-squares analysis[14] to determine the nine components of the **g** and hyperfine tensors given in Table III. The least-squares fit included corrections to second order in perturbation theory. The least-squares parameters were used to generate the simulated spectrum shown in Figure 3b.[7] The agreement between experimental and simulated spectra is satisfactory; the several small discrepancies seem to be due to variable component widths in the experimental spectrum that may arise from exchange of the phosphine ligand between sites of large and small ^{31}P coupling or possibly from small unresolved quadrupolar splittings.

Up to this point, it was assumed that the **g** tensor and hyperfine tensors share principal axes. This assumption appears to be justified for the **g** tensor and the ^{59}Co hyperfine tensor; the least-squares fit became significantly worse when even small angles were assumed between the principal axes of these tensors. Because the ^{31}P hyperfine tensor is so nearly isotropic, the orientations of its principal axes are more difficult to pin down. The spectrum can be fitted for ^{31}P hyperfine tensor principal axes differing from the **g** tensor axes by up to about 30°. Although the ^{31}P tensor components so obtained depend on the assumed orientation of the axes, the **g** tensor and ^{59}Co hyperfine tensor components are quite insensitive and simulated spectra are virtually superimposable. Thus, we can say only that the ^{31}P tensor axes are within about 30° of the **g** tensor axes and that the major axes of both hyperfine tensors (i.e., the largest ^{31}P and the positive ^{59}Co components) are approximately colinear.

Other frozen-solution spectra were qualitatively similar to that described above. In those cases where spectral features can be assigned with certainty, the **g** tensor and ^{59}Co nuclear hyperfine tensor components differ only slightly from those given in Table III. Spectra of the di- and trisubstituted radicals are considerably more complex. There is some indication that the fluxional behavior responsible for the line width effects described above is still fast enough at 120–140 K to cause the features from some nuclear spin states to be in the fast-exchange limit, some to be in the slow-exchange limit, and some to be in the intermediate-exchange region. Although series of features can still be identified that permit determination of the two largest ^{59}Co hyperfine tensor components (which are similar to those given in Table III), determination of the ^{31}P hyperfine tensor is not possible. Experiments at liquid-helium temperature are planned.

Discussion

Identity of the Radicals. We have assumed in this paper, up to this point without proof, that the spectra described here are due to radicals of the general formula $(RCCR')Co(CO)_{3-x}L_x$. This identification is based on a number of pieces of circumstantial evidence that we will now review. (1) Since all 19 spectra reported here give similar g values and ^{59}Co coupling constants, it is reasonable to conclude that the radicals are structurally similar. (2) Since the ESR parameters depend on the acetylene substituents, the acetylene moiety must be included in the radicals. No organic products other than the acetylene were detected in the electrochemical experiments.[8] (3) Since spectra with zero, one, two, and three ^{31}P couplings have been observed, we conclude that there are three carbonyl or Lewis base ligands in addition to the acetylene. (4) The frozen-solution spectra reported here are qualitatively similar to that of $(Ph_2C_2)Co(PMe_3)_3$, which was produced and characterized by more conventional techniques.[15] (5) The formulation assumed here enabled us to provide a coherent explanation of the electrochemical results reported earlier[8] and to correlate those results with radical yields and lifetimes observed in the ESR experiments. (6) Conclusions regarding electronic structure and fluxional behavior (to be discussed below) are consistent with the assumed formula.

Interpretation of ESR Parameters. The ^{59}Co hyperfine tensor is very anisotropic but has principal axes that are coincident with the **g** tensor principal axes. These conditions restrict cobalt 3d contributions to combinations of d_{z^2} and $d_{x^2-y^2}$ orbitals. Other hybridization schemes would result in either an axial tensor or noncoincident tensor axes.[7] Thus, if the semioccupied molecular orbital (SOMO) is

$$\psi_{SOMO} = a|z^2\rangle + b|x^2 - y^2\rangle + \ldots \quad (4)$$

then the hyperfine tensor components, including spin–orbit contributions, are given by[16]

$$A_i = [\kappa_s\rho^{4s} - \kappa_p\rho^{3d} + \alpha_i + \Delta g_i]P \quad (5)$$

where $\Delta g_i = g_i - g_e$, ρ^{4s} and $\rho^{3d} = a^2 + b^2$ are the 4s and 3d spin densities, κ_s and κ_p are the Fermi contact contributions from 4s spin density and polarization of inner-shell s orbitals,

(14) Rieger, P. H. *J. Magn. Reson.* **1982**, *50*, 485–489.

(15) Klein, H. F. *Angew. Chem.* **1980**, *92*, 362–375.

(16) McGarvey, B. R. In "Electron Spin Resonance of Metal Complexes"; Yen, T. F., Ed.; Plenum Press: New York, 1969; pp 1–11.

Table IV. Cobalt AO Contribution to SOMO

ρ^{3d}	% d_{z^2}	assgnt[a] (x, y, z)	ρ^{3d}	% d_{z^2}	assgnt[a] (x, y, z)
0.636	98.2	1, 2, 3	0.630	11.2	2, 3, 1
0.620	41.8	1, 3, 2			

[a] Assignment of molecular axes to tensor components listed in Table III.

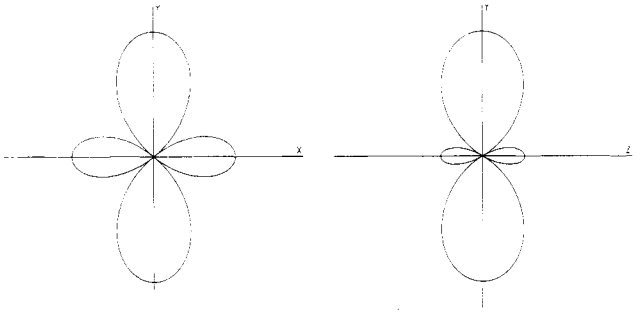

Figure 4. Polar plots of 11.2% d_{z^2} −88.8% $d_{x^2-y^2}$ hybrid orbitals.

respectively, and $P = g_e g_N \mu_B \mu_N \langle r^{-3} \rangle$. The dipolar contributions α_i are given by[16]

$$\alpha_x = -\frac{2}{7}(a^2 - b^2) - \frac{4(3^{1/2})}{7}ab(1 + \Delta g_z/8b^2) + \frac{1}{14}\left(\frac{3^{1/2}a + b}{3^{1/2}a - b}\right)\Delta g_y \quad (6a)$$

$$\alpha_y = -\frac{2}{7}(a^2 - b^2) + \frac{4(3^{1/2})}{7}ab(1 + \Delta g_z/8b^2) + \frac{1}{14}\left(\frac{3^{1/2}a - b}{3^{1/2}a + b}\right)\Delta g_x \quad (6b)$$

$$\alpha_z = \frac{4}{7}(a^2 - b^2) - \frac{1}{14}\left(\frac{3^{1/2}a + b}{3^{1/2}a - b}\right)\Delta g_y - \frac{1}{14}\left(\frac{3^{1/2}a - b}{3^{1/2}a + b}\right)\Delta g_x \quad (6c)$$

and the **g** tensor anisotropies are[16]

$$\Delta g_x = (3^{1/2}a + b)^2(\lambda/\Delta E_{yz}) \quad (7a)$$

$$\Delta g_y = (3^{1/2}a - b)^2(\lambda/\Delta E_{xz}) \quad (7b)$$

$$\Delta g_z = 4b^2(\lambda/\Delta E_{xz}) \quad (7c)$$

where λ is the spin–orbit coupling parameter (ca. 1034 cm^{-1} for Co(O))[17] and ΔE_i is the energy difference between the SOMO and the specified d orbital. Since there may be several MO's with d_{xz} character (for example), these energy differences are really weighted averages and must be interpreted with caution.

The signs of the ^{59}Co hyperfine couplings listed in Tables I and III are based on the expectation that the isotropic coupling is due largely to polarization of inner-shell s orbitals, $\kappa_s\rho^{4s} < \kappa_p\rho^{3d}$, and is therefore negative. The ^{31}P couplings, on the other hand, are assumed positive on the expectation that the isotropic coupling arises largely from phosphorus 3s spin density.

The experimental ^{59}Co hyperfine tensor and **g** tensor components given in Table III can be fitted to eq 5–7 by using $P = 0.0228$ cm^{-1}.[18] Six different assignments are possible of the three tensor components to the molecular x, y, and z axes. With the hybrid orbital major axis assumed to be the molecular z axis, then the cobalt 3d contribution is about 98% d_{z^2}. On the other hand, if the major axis is x or y, then the d_{z^2} contribution could be 42% or 11%. The three assignments that correspond to $a/b > 0$ are given in Table IV. The assignments for $a/b < 0$ are identical except that the x and y axes are interchanged. With the estimates of ρ^{3d} given in Table IV, $\kappa_s P = 0.1938$ cm^{-1},[18] and $\kappa_p P = 0.0094$ cm^{-1},[7] the 4s contribution to the SOMO is found to be quite negligible, less than 0.003 for all possible assignments.

It is important to note that it is the shape of the SOMO that is determined by the ESR parameters. Polar plots of the orbital with 11.2% d_{z^2} character are shown in Figure 4 for projections in the xy and yz planes. The orbital resembles d_{z^2} but with a distorted equatorial doughnut. The major axis in this case is y, but other choices of a and b would give orbitals of virtually the same shape but with major axes along x or z.

The isotropic ^{31}P coupling in $(t\text{-}Bu_2C_2)Co(CO)_2P\text{-}n\text{-}Bu_3$ arises largely through 3s spin density on phosphorus. The observed coupling is large and almost certainly positive so that it is reasonable to neglect inner-shell s-orbital polarization. Taking $\kappa_s P = 0.444$ cm^{-1} [19] and neglecting spin–orbit contributions, we have $\rho^{3s} = 0.025$.

The anisotropic part of the ^{31}P hyperfine interaction is more complicated. Possible contributions arise from the dipolar coupling of the ^{31}P nucleus with (i) positive spin density in the phosphorus $3p_z$ orbital, (ii) negative spin density in the $3p_x$ and/or $3p_y$ orbitals resulting from polarization of the occupied CoP π orbitals by spin density on cobalt, and (iii) direct dipolar coupling with spin density on cobalt. The last effect is expected to have a principal value on the order of 1×10^{-4} cm^{-1} and can be neglected here without serious error.[20] Labauze and Raynor[22] have shown that spin polarization of Co–P bonds is not negligible; indeed, contributions i and ii may be of comparable magnitude. The anisotropic part of the hyperfine tensor may be decomposed[22] into an axial component with principal value 13.8×10^{-4} cm^{-1} associated with the major axis (contribution i) and a second axial component with a principal value -4.2×10^{-4} cm^{-1} associated with an axis perpendicular to the major axis (contribution ii).[23] For spin density in a phosphorus 3p orbital, the major dipolar hyperfine component is expected to be $^4/_5 P\rho^{3p}$. With $P = 0.0306$ cm^{-1},[19] we have $\rho^{3p} = 0.056$, giving a 3p:3s hybridization ratio of 2.2. Labauze and Raynor[22] obtained hybridization ratios of 1.4 to 1.9 for $P\text{-}n\text{-}Bu_3$ in a series of Schiff base low-spin Co(II) complexes. Since the ^{31}P hyperfine tensor obtained for assumed noncoincident tensor axes gives a hybridization ratio of up to 3.3,

(17) Goodman, B. A.; Raynor, J. B. *Adv. Inorg. Chem. Radiochem.* **1970**, *13*, 135–362.

(18) Morton and Preston[19] give $P = 0.0282$ cm^{-1} for cobalt, presumably in the $3d^74s^2$ ground state. Goodman and Raynor[17] give $P = 0.0250$ cm^{-1} for $3d^74s^2$ and $P = 0.0202$ cm^{-1} for $3d^9$. Assuming that the Morton and Preston value is more accurate for the atomic ground state, that the $3d^9$ configuration is more appropriate here, and that the ratio of the Goodman and Raynor values is approximately correct, we obtain $P = 0.0228$ cm^{-1}.

(19) Morton, J. R.; Preston, K. F. *J. Magn. Reson.* **1978**, *30*, 577 582.

(20) This result is based on calculations using the methods of McConnell and Strathdee[21]; see also ref 22.

(21) McConnell, H. M.; Strathdee, J. *Mol. Phys.* **1959**, *2*, 129–138.

(22) Labauze, G.; Raynor, J. B. *J. Chem. Soc., Dalton Trans.* **1980**, 2388–2394; **1981**, 590–598.

(23) The apparent anisotropy of the ^{31}P hyperfine tensor is strongly dependent on the assumed orientation of the principal axes. Analysis of the ESR spectrum suggests that the major axes of the ^{59}Co and ^{31}P hyperfine tensors are separated by less than 30°. The ^{31}P hyperfine components given in Table III correspond to coincident tensor axes, but, within experimental error, the major component of the ^{31}P hyperfine tensor may be as large as 138×10^{-4} cm^{-1}, while one of the other components may be as small as 93×10^{-4} cm^{-1}. When the dipolar tensor is decomposed into two axial tensors, the positive parallel component might be as large as 20×10^{-4} cm^{-1} and the negative value anywhere from 0 to -10×10^{-4} cm^{-1}

it seems likely that angle between the major hyperfine axes is indeed near zero.

The ^{31}P isotropic couplings observed for the radicals containing phosphite ligands are substantially larger than those containing phosphines. Although the hyperfine tensors cannot be accurately determined from the frozen-solution spectra of the phosphite radicals, the anisotropy appears to be no larger than in the case of the P-*n*-Bu_3 radical. This would suggest that the 3p:3s hybridization ratio is substantially smaller for phosphites, consistent with observation on other systems.[22,24,25]

If the Co–P bond in (*t*-Bu_2C_2)Co(CO)$_2$P-*n*-Bu_3 lies along the major axis of the SOMO, it is reasonable to suppose that the unique phosphorus ligand in the di- and trisubstituted radicals occupies a similar position. The ligands giving smaller ^{31}P couplings then are presumably in a plane perpendicular to this axis. The isotropic ^{31}P couplings estimated for the P(OMe)$_3$-substituted radicals are 184×10^{-4} cm^{-1} for the site A ligand and 26×10^{-4} cm^{-1} for the site B ligands. These values may be compared with ^{31}P couplings for phosphorus ligands substituted at the axial positions in a series of Schiff base low-spin Co(II) complexes where the unpaired electron is in a Co d_{z^2} orbital; ^{31}P couplings ranged from 148×10^{-4} to 179×10^{-4} cm^{-1} for phosphines and 240×10^{-4} to 273×10^{-4} cm^{-1} for phosphites.[22] Square-planar low-spin Co(diphos)$_2^{2+}$, where the SOMO is again cobalt d_{z^2} gave isotropic ^{31}P couplings ranging from 16.7×10^{-4} to 17.8×10^{-4} cm^{-1}, depending on the counterion.[26] The magnitude and sign of the equatorial ^{31}P couplings are expected to be sensitive to the P_{ax}–Co–P_{eq} angle with a positive value on the order of 20×10^{-4} cm^{-1} for 90°; the coupling should decrease to zero and become negative as the angle increases or decreases and the phosphorus atom approaches the conical node of the cobalt d_{z^2} orbital. The estimated coupling of site B phosphite ligands thus suggests that the P_{ax}–Co–P_{eq} angle is near 90° for the acetylene cobalt radicals.

We have accounted for about 71% of the spin density—63% in cobalt d orbitals and 8% in orbitals of the unique phosphorus atom. Small amounts might be accounted for by the other two ligands and by cobalt 4p contributions, and the Co 3d contribution may be low by 10%,[18] but it seems likely that the acetylene plays a significant role in the SOMO.

Structure of the Radicals. Two limiting structures can be inferred from the relative dispositions of the phosphorus ligands. In an approximate square-planar structure, **1**, the unique

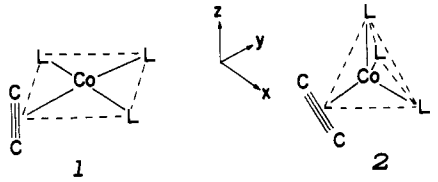

1

2

phosphorus ligand would be trans to the acetylene. If the pseudofourfold axis of **1** is labeled *z*, then the SOMO major axis is *y*, and the SOMO composition is best described by the third entry in Table IV (11% d_{z^2}). In a trigonal-pyramidal structure, **2**, the unique ligand would occupy the apical position. The SOMO major axis is the pseudo-3-fold axis, *z*, and the SOMO composition is described by the first entry in Table IV (98% d_{z^2}).

Several precedents can be found for structure **2**. Co(CO)$_4$, prepared by the cocondensation of Co and CO on a sapphire rod at 6 K[27] or by sublimation of $Co_2(CO)_8$ on a cold finger at 77 K[28] gave an ESR spectrum consistent with a C_{3v} structure. Similarly, ESR spectra of Co[(OMe)$_3$]$_4$[29] and Co[P(Me)$_3$]$_4$[14] showed axial **g** and ^{59}Co hyperfine tensors and unique ^{31}P nuclei, again suggesting a C_{3v} structure. When one of the ligands in CoL_4 is replaced by an acetylene, there is precedent for a phosphite ligand in the apical position. Thus, the structure of $(Ph_2C_2)Co(PMe_3)_3^+$ is pseudotetrahedral with one phosphine ligand significantly more tightly bound.[30] In this case, however, the acetylene apparently acts as a four-electron donor and should probably be regarded as a bidentate ligand; the structure could then be described as square pyramidal with the unique phosphine ligand at the axial coordination site. Similarly, the structures of (η^3-cyclooctenyl)Fe[P(OMe)$_3$]$_3^+$,[31] (η^3-cyclooctenyl)Fe[P(OMe$_3$]$_3$,[31] and (η^3-cyclooctenyl)Co[P(OMe)$_3$]$_3$[31,32] are all approximately square pyramidal with a phosphite ligand at the apical position. The ESR spectrum[33] of the paramagnetic iron complex shows a unique ^{31}P coupling (99.6 G) and two small negative couplings (−27.9 and −10.5 G); fluxional processes average the ^{31}P couplings. The SOMO for the iron radical is a d_{z^2}-like orbital directed toward the unique phosphite ligand[31] and therefore very similar to the SOMO description for the acetylene cobalt radicals if they have structure **2**. It is important to note, however, that the iron radical is a d^7 system whereas the acetylene cobalt radicals are d^9. Thus, if these radicals are structurally similar, the SOMO of the acetylene cobalt radicals would probably be located in the basal plane rather than along the pseudo-3-fold axis. Structure **2** thus appears to be inconsistent with the ESR results.

There are several additional reasons for preferring a structure close to **1**. (1) Since the acetylene apparently makes a significant contribution to the SOMO, it seems reasonable to suppose that the cobalt SOMO contribution overlaps the acetylene π system, i.e., that the acetylene is trans to the strongly coupled ligand. (2) In MO descriptions of olefin or acetylene π complexes,[34] three MO's of a_1 symmetry (in the C_{2v} symmetry of structure **1**) are formed from metal d_{z^2} and $d_{x^2-y^2}$ orbitals and a ligand π orbital. Two of these are low-lying bonding orbitals; the third is an antibonding orbital that is predominantly $d_{x^2-y^2}$ but with significant d_{z^2} and ligand π character. This orbital, which is the LUMO in square-planar d^8 complexes, is the predicted SOMO for d^9 radicals. The description of the SOMO, derived from ESR parameters, is in fact in good agreement with this prediction. (3) MO calculations on Co(CO)$_4$,[35-37] which is isoelectronic with the acetylene cobalt radicals, predict that the ground-state configuration is a D_{2d} structure with C–Co–C bond angles of about 100 and 130°. A distortion of **1** from the limiting square-planar structure to a conformation analogous to D_{2d} Co(CO)$_4$ would be compatible with the ESR results. The C_{3v} structure of Co(CO)$_4$, which is apparently the actual ground state,[27,28] is at only slightly higher energy in the calculations, and at somewhat higher energies are the tetrahedral and square-planar limiting structures to which the C_{3v} and D_{2d} structures

(24) Wayland, B. B.; Abd-Elmageed, M. E.; Mehne, L. F. *Inorg. Chem.* **1975**, *14*, 1456–1460.
(25) Kawamura, T.; Fukamachi, K.; Sowa, T.; Hayashida, S.; Yonezama, T. *J. Am. Chem. Soc.* **1981**, *103*, 364–369.
(26) Attanasio, D. *Chem. Phys. Lett.* **1977**, *49*, 547–549.
(27) Hanlan, L. A.; Huber, H.; Kundig, E. P.; McGarvey, B. R.; Ozin, G. A. *J. Am. Chem. Soc.* **1975**, *97*, 7054–7068.
(28) Fieldhouse, S. A.; Fullam,B. W.; Neilson, G. W.; Symons, M. C. R. *J. Chem. Soc., Dalton Trans.* **1974**, 567–569.
(29) Muetterties, E. L.; Bleeke, J. R.; Yang, Z.-Y.; Day, V. W. *J. Am. Chem. Soc.* **1982**, *104*, 2940–2942.
(30) Capell, B.; Beauchamp, A. L.; Dartiguenave, M.; Dartiguenave, Y. *J. Chem. Soc., Chem. Commun.* **1982**, 566–568.
(31) Harlow, R. L.; McKinney, R. J.; Ittel, S. D. *J. Am. Chem. Soc.* **1979**, *101*, 7496–7504.
(32) Thompson, M. R.; Day, V. W.; Tau, K. D.; Muetterties, E. L. *Inorg. Chem.* **1981**, *20*, 1237–1241.
(33) Ittel, S. D.; Krusic, P. J.; Meakin, R. *J. Am. Chem. Soc.* **1978**, *100*, 3264–3266.
(34) Albright, T. A.; Hoffmann, R.; Thibeault, J. C.; Thorn, D. C. *J. Am. Chem. Soc.* **1979**, *101*, 3801–3812.
(35) Burdett, J. K. *J. Chem. Soc., Faraday Trans. 2* **1974**, 70, 1599–1613.
(36) Elian, M.; Hoffmann, R. *Inorg. Chem.* **1975**, *14*, 1058–1076.
(37) Pensak, D. A.; McKinney, R. J. *Inorg. Chem.* **1979**, *18*, 3407–3417.

are related. In general, four-coordinate d^9 complexes are expected to be stereochemically nonrigid with relatively low barriers between several potential energy minima. Thus, we may expect a readily accessible pathway for intramolecular ligand exchange, consistent with the extremely rapid fluxionality observed in the acetylene cobalt radicals.

Acknowledgment is made to the donors of the Petroleum Research Fund, administered by the American Chemical Society, for partial support of this research both at Brown University and at the University of Otago. We are grateful to the National Science Foundation for assistance in the purchase of an ESR spectrometer by Brown University. We thank P. J. Krusic for helpful discussions and for his encouragement in this work and H. F. Klein for communicating the details of some ESR spectra.

Registry No. $(Ph_2C_2)Co(CO)_3$, 90219-71-9; $(t\text{-}Bu_2C_2)Co(CO)_3$, 90219-72-0; $(Ph_2C_2)Co(CO)_2P\text{-}n\text{-}Bu_3$, 90219-73-1; $(Ph_2C_2)Co(CO)_2P(c\text{-}C_6H_{11})_3$, 90219-74-2; $(Ph_2C_2)Co(CO)_2PPh_3$, 90219-75-3; $(Ph_2C_2)Co(CO)_2P(OMe)_3$, 90245-32-2; $(Ph_2C_2)Co(CO)_2P(OPh)_3$, 90219-76-4; $(Ph_2C_2)Co(CO)_2AsPh_3$, 90219-77-5; $(t\text{-}Bu_2C_2)Co(CO)_2P\text{-}n\text{-}Bu_3$, 90219-78-6; $(t\text{-}Bu_2C_2)Co(CO)_2P(OMe)_3$, 90219-79-7; $[CF_3C_2Si(CH_3)_3]Co(CO)[P(OMe)_3]_2$, 90219-80-0; $[(CF_3)_2C_2]Co(CO)[P(OMe)_3]_2$, 90219-81-1; $(Ph_2C_2)Co(CO)[P(OEt)_3]_2$, 90219-82-2; $(Ph_2C_2)Co(CO)[P(OMe)_3]_2$, 90219-83-3; $(Ph_2C_2)Co(CO)[Ph_2PCH_2CH_2PPh_2]$, 90219-84-4; $(Ph_2C_2)Co(CO)[Ph_2AsCH_2CH_2AsPh_2]$, 90219-85-5; $(Ph_2C_2)Co(CO)[Ph_2PCH_2CH_2AsPh_2]$, 90219-86-6; $[(CF_3)_2C_2]Co[P(OMe)_3]_3$, 90219-87-7; $(Ph_2C_2)Co[P(OMe)_3]_3$, 90219-88-8; $(Ph_2C_2)Co_2(CO)_6$, 14515-69-6; $(t\text{-}Bu_2C_2)Co_2(CO)_6$, 59687-97-7; $[(CF_3)_2C_2]Co_2(CO)_6$, 37685-63-5; $[CF_3C_2Si(CH_3)_3]Co_2(CO)_6$, 38599-40-5; $(Ph_2C_2)Co_4(CO)_{10}$, 11057-43-5; $(Ph_2C_2)Co_2(CO)_3[P(OMe)_3]_3$, 55925-87-6; $[(CF_3)_2C_2]Co_2(CO)_3[P(OMe)_3]_3$, 90219-89-9.

Contribution from the Department of Chemistry, Miami University, Oxford, Ohio 45056

Electronic Structure of $(\mu\text{-H})Cr_2(CO)_{10}^-$

CHARLES J. EYERMANN and ALICE CHUNG-PHILLIPS*

Received October 18, 1983

Ground-state self-consistent-field Xα scattered-wave (SCF-Xα-SW) calculations have been carried out for the dinuclear transition-metal hydride complex $(\mu\text{-H})Cr_2(CO)_{10}^-$. Valence energy levels and sphere charge distributions, core energy levels, and total energies and sphere charges are obtained. The principal MO describing the Cr–H–Cr bond, $15a_1$, is predominantly H ligand in character. Other MOs with noticeable H ligand character include $7a_1$, $8a_1$, $9a_1$, and $14a_1$. These findings indicate that the bonding scheme for the Cr–H–Cr linkage is more complex than the qualitative three-center two-electron bond previously proposed. One of the two highest occupied MOs, $16b_1$, is Cr–Cr antibonding and $Cr–CO_t$ bonding where CO_t refers to the trans carbonyl. The lowest lying virtual orbital, $18a_1$, is Cr–Cr bonding but both $Cr–CO_t$ and $H–Cr_2$ antibonding. The lowest energy electronic transition, $16b_1 \rightarrow 18a_1$, is therefore expected to produce an excited state that is conducive to a facile CO dissociation but is not favorable to the disruption of the Cr–H–Cr bridging framework. This excited state is consistent with the high quantum yield observed for the photosubstitution of CO and the low quantum yield for photoinduced dimer disruption.

Introduction

In 1970, the geometry of the non-hydrogen framework in the anion of $[Et_4N^+][(\mu\text{-H})Cr_2(CO)_{10}^-]$, determined by X-ray diffraction,[1] was used to postulate a linear M–H–M bridging unit, **1**, where M designates the metal. However, X-ray and

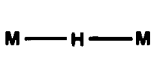

1

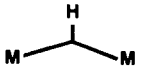

2

subsequent neutron diffraction investigations[2] on $(\mu\text{-H})W_2(CO)_9NO$ supplied the first direct evidence that unsupported M–H–M linkages are inherently bent, **2**. Indeed, a reinvestigation of $[Et_4N^+][(\mu\text{-H})Cr_2(CO)_{10}^-]$ using neutron diffraction revealed the H ligand position to be ca. 0.3 Å above the Cr–Cr internuclear axis;[3] i.e., the Cr–H–Cr fragment in this complex is *bent* and not linear as originally suggested. Additional X-ray and neutron diffraction studies have reaffirmed the bent configuration of M–H–M and have also shown that M–H–M bond angles may vary from 85 to 159°.[4] For example, the Et_4N^+ and Ph_4P^+ salts of $(\mu\text{-H})W_2(CO)_{10}^-$ have W–H–W bond angles of 137 and 123°, respectively.[4c] The highly variable M–H–M angle suggests an easily deformable M–H–M bridge.

Based on the neutron diffraction study[2b] of $(\mu\text{-H})W_2(CO)_9NO$, the H position is displaced outward from (**3**), rather than at (**4**), the intersection of the metal–axial-ligand (M–L) bond vectors. The observation has led to the supposition that

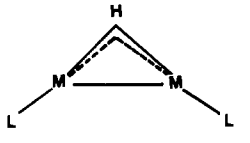

3

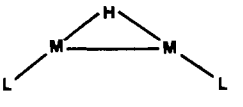

4

the M–H–M bond is best described as a closed (**5**), rather than an open (**6**), three-center two-electron (3c, 2e) bond.

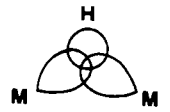

5

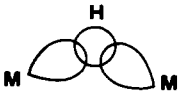

6

(1) Handy, L. B.; Ruff, J. K.; Dahl, L. F. *J. Am. Chem. Soc.* **1970**, *92*, 7312.

(2) (a) Andrews, M. A.; Tipton, D. L.; Kirtley, S. W.; Bau, R. *J. Chem. Soc., Chem. Commun.* **1973**, 181. (b) Olsen, J. P.; Koetzle, T. F.; Kirtly, S. W.; Andrews, M. A.; Tipton, D. L.; Bau, R. *J. Am. Chem. Soc.* **1974**, *96*, 6621.

(3) Roziere, J.; Williams, J. M.; Stewart, R. P., Jr.; Petersen, J. L.; Dahl, L. F. *J. Am. Chem. Soc.* **1977**, *99*, 4497.

(4) (a) Petersen, J. L.; Johnson, P. L.; O'Connor, J.; Dahl, L. F. *Inorg. Chem.* **1978**, *17*, 3460. (b) Petersen, J. L.; Brown, R. K.; Williams, J. M.; McMullan, R. K. *Ibid.* **1979**, *18*, 3493. (c) See references cited in: Bau, R.; Teller, R. G. *Struct. Bonding (Berlin)* **1981**, *44*, 1.

0020-1669/84/1323-2025$01.50/0